J Mater Sci: Mater Med (2012) 23:51–61
DOI 10.1007/s10856-011-4505-2

Hydroxyapatite/gelatin/gellan sponges as nanocomposite scaffolds for bone reconstruction

Niccoletta Barbani · Giulio D. Guerra · Caterina Cristallini · Patrizia Urciuoli · Riccardo Avvisati · Alessandro Sala · Elisabetta Rosellini

Received: 1 August 2011 / Accepted: 16 November 2011 / Published online: 25 November 2011

Abstract The aim of this work was the morphological, physicochemical, mechanical and biological characterization of a new composite system, based on gelatin, gellan and hydroxyapatite, and mimicking the composition of natural bone. Porous scaffolds were prepared by freeze–drying technique, under three different conditions of freezing. The morphological analysis showed a homogeneous porosity, with well interconnected pores, for the sample which underwent a more rapid freezing. The elastic modulus of the same sample was close to that of the natural bone. The presence of interactions among the components was demonstrated through the physicochemical investigation. In addition, the infrared chemical imaging analysis pointed out the similarity among the composite scaffold and the natural bone, in terms of chemical composition, homogeneity, molecular interactions and structural conformation. Preliminary biological characterization showed a good adhesion and proliferation of human mesenchymal stem cells.

N. Barbani (✉) · R. Avvisati · A. Sala · E. Rosellini (✉)
Department of Chemical Engineering, Industrial Chemistry and Materials Science, University of Pisa, Largo Lucio Lazzarino, 56122 Pisa, Italy
e-mail: n.barbani@diccism.unipi.it

E. Rosellini
e-mail: elisabetta.rosellini@diccism.unipi.it

G. D. Guerra · C. Cristallini
Institute for Composite and Biomedical Materials, C.N.R., U.O.S. of Pisa, Largo Lucio Lazzarino, 56122 Pisa, Italy

P. Urciuoli
Cell Biology and Tissue Regeneration Laboratory, Immunohematology 2 Unit, Azienda Ospedaliera Universitaria Pisana, Via Paradisa 1, 56124 Pisa, Italy

1 Introduction

Collagen (Col) and hydroxyapatite (HA) are widely investigated materials for the realization of biomimetic scaffolds that promote new bone formation, because their composites resemble the structure of natural bone tissue [1], showing excellent bioactivity and osteoconductivity [2–6]. The performance of these nanocomposite scaffolds relies on the relationship between the role played by the polymer interactions of the matrix and the cell and tissue compatibility of the resulting materials. The study and the comprehension of the interactions at molecular level is of fundamental importance for a selection, at a very early stage, of the more promising polymers aimed at realising new systems with improved performances. Recently, gelatin (Gel), which is the denatured form of Col, was found to be an attractive component for the replacement of the extracellular matrix, since it contains several functional groups, which enhance osteoblast adhesion and migration. However, since Gel lacks the structural characteristics of Col, HA–Gel scaffolds have poor mechanical properties; consequently, various procedures have been used to improve them, like additional fillers, functional group grafting, chemical cross-linking [7].

In this work, our aim is to investigate the morphological, physicochemical, mechanical and biological properties of a new polymeric system, based on gellan gum (GE), Gel and HA and mimicking the composition of natural bones. Since Gel is the denatured form of Col, its interactions with HA are very similar to those found in the HA–Col composites [2, 3, 8]. Composites between GE and HA were prepared and examined by the authors' research team some years ago, in view of their possible use to make scaffolds for bone regeneration. The formation of ionic bonds between the Ca^{2+} ions in the HA lattice and the carboxyl groups

present in the glucuronic acid units of the GE chain was ascertained [5, 9]; these bonds are shown in Fig. 1. It was also reported that the addition of GE to Gel could improve the mechanical properties of the resulting material; this fact was attributed to the interactions between the carboxylate groups of GE and the amide I groups of Gel [10]. An additional very strong interaction between the two macromolecules can be the ionic bond between the carboxyl group of the GE repeating unit and the side amino group of a basic amino acid of the Gel peptide chain, like lysine, as shown in Fig. 2. The Gel chains have been cross-linked, condensing glutamine residues with polypeptide units of amino acids containing side amino groups, as shown in Fig. 3, by the action of the enzymatic catalyst transglutaminase (TGase). This technique mimics in vitro the enzymatic cross-linking reactions mediated by TGase, which occur naturally in the body [11]. The trans-amidation reaction produced by the enzyme was used by us [4, 6] and by other authors [12] to cross-link Col; in particular, it was found that the so cross-linked Col undergoes cell attachment, spreading and proliferation of human osteoblasts and human foreskin dermal fibroblasts better than the not cross-linked one [12]. However, only few studies, regarding the use of Gel cross-linked with TGase for tissue engineering, have been reported recently; in particular, an Italian research group used this biomaterial to make scaffolds, on which hepatocytes were successfully seeded in view of liver tissue regeneration [13, 14]. In a previous work, Gel cross-linked with TGase and embedded in a GE matrix was successfully seeded with fibroblasts NIH 3T3, as a preliminary test for soft tissue engineering [15].

In addition to the chemical composition, another aspect that has to be taken in consideration in the development of scaffolds for tissue regeneration is the three dimensional structure. The presence of a good porosity, with well-interconnected pores, is necessary to promote the infiltration of cells, nerves and blood capillaries. Being bone defects subjected to mechanical compression, it is also requested that the presence of pores is combined with an appropriate mechanical resistance. In this work, porous scaffolds were fabricated by freeze–drying process and three different conditions of freezing were tested, to

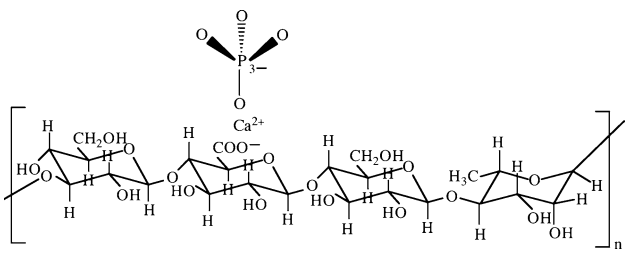

Fig. 1 Scheme of the ionic interaction between a GE carboxyl group and the ionic structure of HA

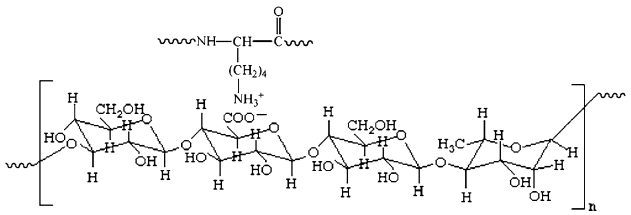

Fig. 2 Scheme of the ionic interaction between a GE carboxyl group and the amino side group of a lysine unit of Gel

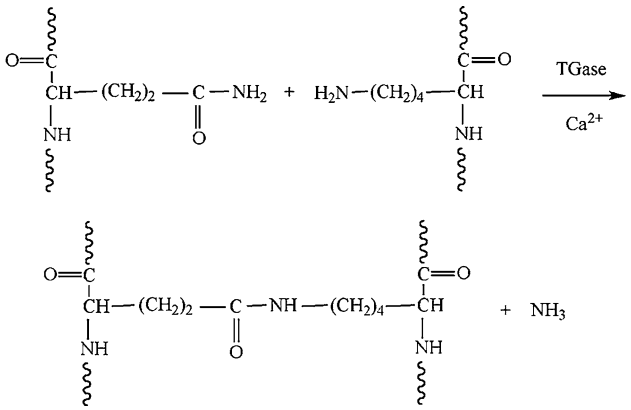

Fig. 3 Scheme of the Gel cross-linking by the enzymatic condensation, catalysed by TGase, of a glutamine residue with a lysine residue

investigate the effect of freezing rate on scaffold morphology.

Scaffolds were then examined by means of morphological, physicochemical, mechanical and cell culture characterization, to test their ability for bone tissue engineering.

2 Experimental

2.1 Scaffold preparation

Soluble porcine Type A Gel, TGase from guinea pig liver and GE were purchased by Sigma (St. Louis, MO, USA). HA, synthesized and thermally treated at 1,100°C with the procedure reported in a previous paper [3], was kindly supplied by ISTEC-CNR, Institute of Science and Technology for Ceramics (Faenza, Italy). 1% (w/v) Gel and GE solutions in water were obtained under mild stirring at 60°C. GE and Gel solutions were mixed in Petri dishes, to obtain a blend containing 0.8 mg of GE per mg of Gel. HA was then added to the natural polymer solution under vigorous stirring, so that Gel to HA weight ratio was equal to 20/80, close to the mean Col to HA ratio in natural bone [1]. The samples were then dried using the freeze–drying technique. With this process, the diameter, shape and interconnectivity of the pores is regulated through the

control of ice crystal growth. Therefore, we tested three different conditions of freezing, to investigate the effect of freezing rate on scaffold morphology: cooling at 4°C, in order to allow GE and Gel gelling, and subsequent freezing at −25°C (hereafter indicated as F1 treatment); freezing at −25°C (F2) and freezing by immersion in liquid nitrogen (F3). The different freezing rates permitted the formation of ice crystals of different dimensions.

The obtained sponges were immersed in a $CaCl_2$ (2% w/v) solution for 2 h for GE cross-linking and washed to remove calcium ions in excess. In order to cross-link Gel, the samples were incubated in a solution of TGase (0.05 U/mg of Gel), in Tris/HCl 100 mM buffer of pH 6.5, containing $CaCl_2$ 0.6 mM as the co-catalyst for mammalian TGase [16, 17], washed and finally freeze–dried. The scheme of Gel enzymatic cross-linking by TGase is represented in Fig. 3.

2.2 Morphological analysis

Scanning electron microscope (SEM JSM 5600, Jeol Ltd) was used in order to investigate the morphology of the samples. The samples were prepared by fracturing the sponges in liquid nitrogen. Before analysis, the samples were mounted on metal stubs and sprayed with gold to a thickness of 200–500 Å using a gold splutter.

Optical microscopy images were also acquired by means of the optical microscope present in the Fourier transformed infrared (FT-IR) spectroscopy apparatus (Perkin Elmer Spectrum One FT-IR Spectrometer).

2.3 Differential scanning calorimetry (DSC)

DSC analysis was performed in the range of 30–300°C using a DSC 7 (Perkin Elmer). The samples were weighted and placed into aluminium pans and heated at the rate of 10°C/min, under nitrogen flow (25 ml/min), with an empty pan as reference. The temperatures and the enthalpies related to the thermal events were measured using the DSC 7 software.

All tests were carried out in triplicate. The results are the mean (±standard error) of three determinations.

2.4 Mechanical characterization

Mechanical tests were performed by the Dynamic Mechanical Analyzer DMA 8000 PerkinElmer. Rectangular samples were prepared with fixed dimensions (10×5 mm^2) and a thickness of 4 mm.

Preliminary tests were performed applying a fixed strain (0.2%) in bending at different frequencies for 30 min at constant temperature (37°C), in order to evaluate if differences in elastic modulus occurred. Frequencies were varied in the range from 1 to 5 Hz.

All tests were carried out in triplicate. The results are the mean (±standard error) of three determinations.

2.5 Infrared spectroscopy studies

2.5.1 Attenuated total reflectance (ATR) FT-IR spectroscopy analysis

Infrared spectra were acquired with a Perkin Elmer Spectrum One FT-IR Spectrometer, equipped with ATR objective lens with a penetration depth of less than 1 μm. All spectra were obtained in the middle range (4,000–710 cm^{-1}) with a resolution of 4 cm^{-1} and representing the average of 16 scans.

2.5.2 Infrared imaging

Spectral images were acquired in transmission and in μATR mode using the infrared imaging system Spotlight 300 (Perkin Elmer). The spectral resolution was 4 cm^{-1}. The spatial resolution was 100×100 μm in μATR mode and 6.25 μm in transmission. Background scans were obtained from a region of no sample. IR images were acquired with a liquid nitrogen cooled mercury cadmium telluride line detector composed of 16 pixel elements. Each absorbance spectrum composing the IR images, and resulting of 16 scans, was recorded for each pixel in the μATR mode using the Spotlight software. Spectra were collected by touching the ATR objective on the sample and collecting the spectrum generated from the surface layer of the sample. The Spotlight software used for the acquisition was also used to pre-process the spectra. IR spectral images were produced by using the absorbance in a given frequency range, 4,000–720 cm^{-1}. Spectra contained in the spectral images were analysed using a compare correlation image. The obtained correlation map indicates the areas of an image where the spectra are most similar to a reference spectrum.

2.6 Isolation and expansion of human mesenchymal stem cells (hMSCs)

Nucleated cells, obtained from Wharton Jelly of umbilical cord (WJC), were plated at 10^5 cells/cm^2 in 25 cm^2 flasks (Sarstedt, Nümbrecht, Germany) and incubated at 37°C with 5% CO_2. After 24 h, the non adherent cells were removed by washing with PBS and fresh medium was added twice a week for about 14 days or until adherent cell reached 90% confluence. A number of cells sufficient for scaffold seeding was obtained after 21 days.

2.7 FACS analysis

WJCs were analyzed for epitope expression using a Cytofluorimeter FACScan (Becton-Dickinson, San Jose,

CA, USA). Cells were detached by trypsinization, centrifuged, resuspended in PBS (Euroclone, Milano, Italy) at 0.5×10^6 cells/ml and stained according to the manufacturer's recommendations with the following monoclonal anti-human antibodies: MHCI (Serotec, Oxford, UK), MHCII (Serotec), CD45 (BD Biosciences, San Jose, CA, USA), CD44 (Chemicon International, Temecula, CA, USA), CD29 (Chemicon International), CD34 (BD Biosciences), CD90 (Santa Cruz Biotechnology, Santa Cruz, CA, USA).

2.8 Cell seeding and induction of osteogenic differentiation

Scaffolds were seeded with approximate density of 10^6 cells/cm^2 and cultured for 15 days in an incubator (37°C, 5% CO_2). Part of them were incubated with osteogenic differentiation medium containing Dulbecco's Modified Eagle's Medium (DMEM) supplemented with 20% foetal calf serum (FCS), 100 U/ml Penicillin, 100 μg/ml Streptomycin, 2 mM L-glutamine, 20 mM β-glycerol phosphate (Sigma), 100 nM dexamethasone (Sigma) and 250 μM ascorbate 2-phosphate (Sigma) and the other part only with DMEM supplemented with 10% FCS as a control. The medium was changed every 3 days.

2.9 Histological analysis

Biomaterials with differentiated cells were fixed in 10 wt% neutral buffered formalin solution and dehydrated, immersed in xylene and embedded in paraffin. The samples were sectioned, then slides were deparaffinized, rehydrated in xylene and microwaved in 10 mmol/l buffer. Samples were stained by haematoxylin and eosin for the histological investigation by optical microscopy.

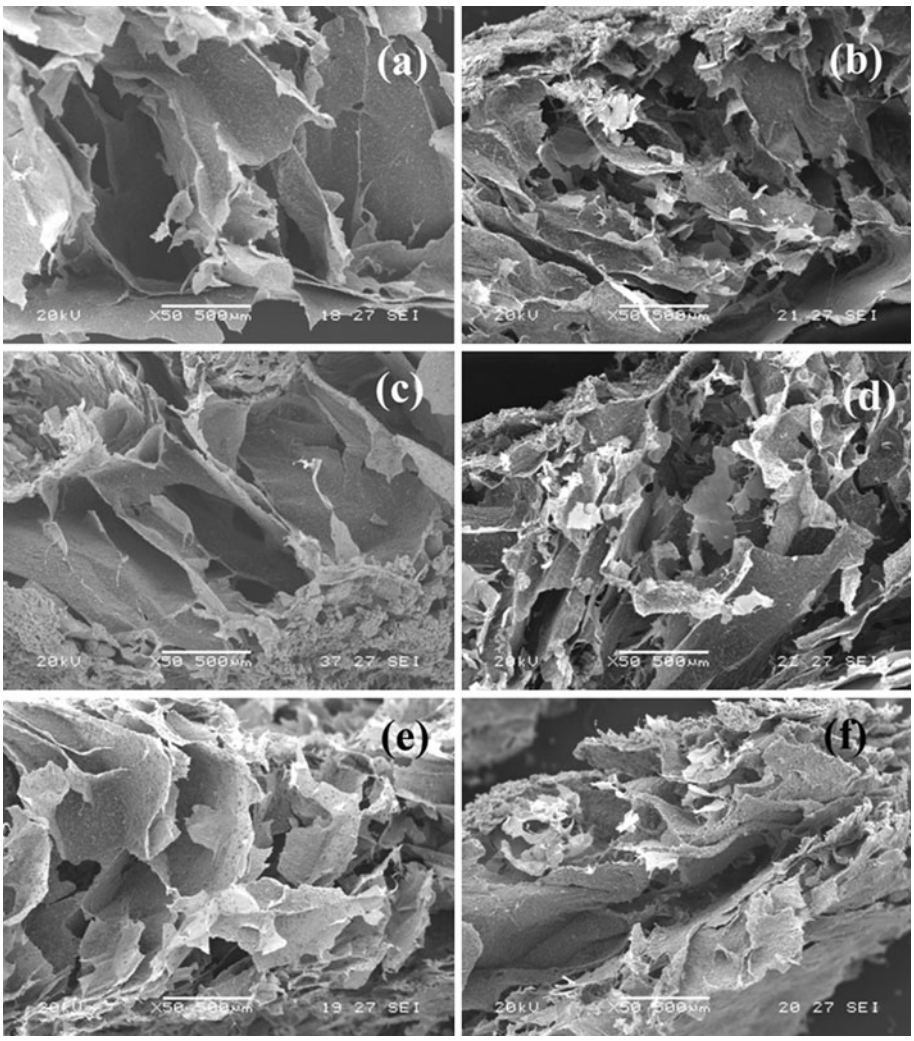

Fig. 4 SEM micrographs of sponges not cross-linked (*left column*) and cross-linked with TGase (*right column*), obtained under different freezing conditions: F1 (**a**, **b**), F2 (**c**, **d**), F3 (**e**, **f**). The micrographs were taken on fracture surfaces parallel to the axes of the sponge cylinders

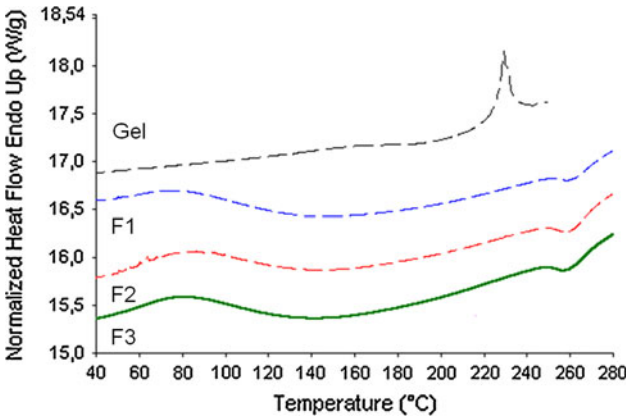

Fig. 5 DSC thermograms of the non cross-linked sponges. The thermograms are compared with that of pure Gel

Table 1 Calorimetric data of F1–F3 samples, compared with pure GE

Sample	T_d (°C)	ΔH (J/g)
F1	260 ± 3	−107 ± 5
F2	260 ± 2	−92 ± 4
F3	262 ± 4	−86 ± 4
GE	249 ± 3	−160 ± 7

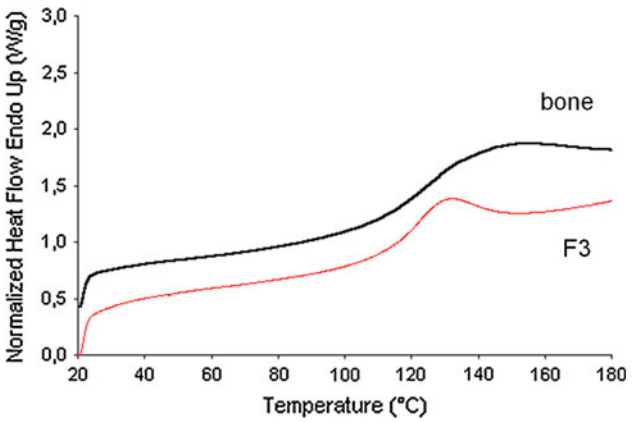

Fig. 6 DSC themograms of the F3 sponge, cross-linked with TGase, and of natural bone

3 Results and discussion

3.1 Morphological analysis

SEM micrographs of sponge fracture surfaces, parallel to the axes of the sponge cylinders, are shown in Fig. 4. A high macro and micro-porosity with a good degree of interconnection was present, tighter in the cross-linked sponges than in the not cross-linked ones. As regarding the latter, the sample F3 (Fig. 4e) resulted more uniform than those obtained with the other procedures (Fig. 4a, c). In particular, for the sample F3, we did not observe a deposition of HA on the inferior surface, that conversely occurred for the samples F1 and F2. Moreover, the sample F3 showed smaller pores, as a consequence of the preparation technique. In the freeze–drying process, pore size is in fact controlled by the size of the ice crystals, which could be adjusted by varying the rate of freezing. In liquid N_2 the freezing process is particularly rapid, with the formation of many ice crystals of small dimensions; since the ice crystals take the action of a template, their shape is imprinted in the porous scaffolds after the drying treatment. A reduction of pores dimension was also observed for all the samples after the cross-linking treatment. All the preformed scaffolds were in fact cross-linked with TGase performing the same treatment, which had the same effect on porosity for all the samples: a contraction of the material and consequently a reduction of pores dimensions. However, even after the cross-linking treatment, the porosity of the scaffolds seems to be appropriate for promoting the adhesion and the proliferation of human osteoblasts, both in vitro and in vivo, being the optimal pore dimensions for hard tissues among 100 and 400 μm [18, 19].

Table 2 Young's Modulus values (E) for HA/Gel/GE sponges, prepared under different freezing conditions, not cross-linked (no TGase) and cross-linked (TGase) by the treatment with TGase in the presence of calcium ions

Sample	E (Pa)	
	No TGase	TGase
F1	$(1.44 \pm 0.09) \times 10^5$	$(2.32 \pm 0.12) \times 10^5$
F2	$(1.86 \pm 0.11) \times 10^5$	$(3.67 \pm 0.19) \times 10^5$
F3	$(5.46 \pm 0.32) \times 10^5$	$(1.79 \pm 0.09) \times 10^6$

The Young's modulus of natural bone was 20–500 MPa [27]

3.2 Differential scanning calorimetry

The DSC thermograms of the sponges obtained under the three different freezing conditions were compared with those of Gel and GE (Fig. 5). The thermograms of the non cross-linked scaffolds showed an endothermic event among 30 and 120°C, due to the evaporation of residual water present in the samples. Moreover, an exothermic event due to the degradation of the polysaccharide was observed. However, in the scaffolds thermograms, the GE degradation event was weakened and shifted toward higher temperatures with respect to the pure polysaccharide (Table 1). The stabilization of the polysaccharide from the thermodegradative point of view was particularly evident for the sample F3. In addition, the glass transition event of Gel (220°C) was not evident, as a consequence of the

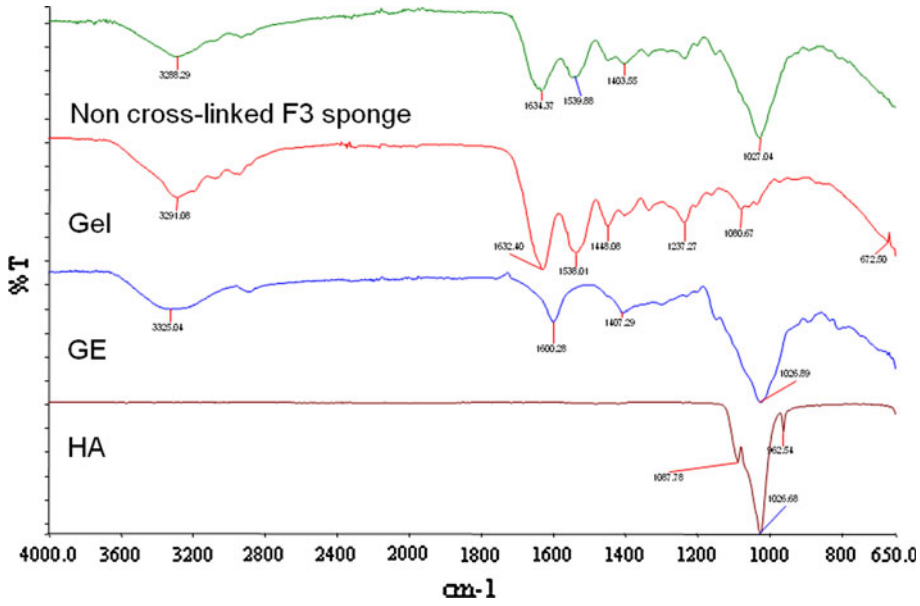

Fig. 7 Infrared spectra acquired in ATR mode for *Gel*, *GE*, *HA* and *non cross-linked F3 sponge*

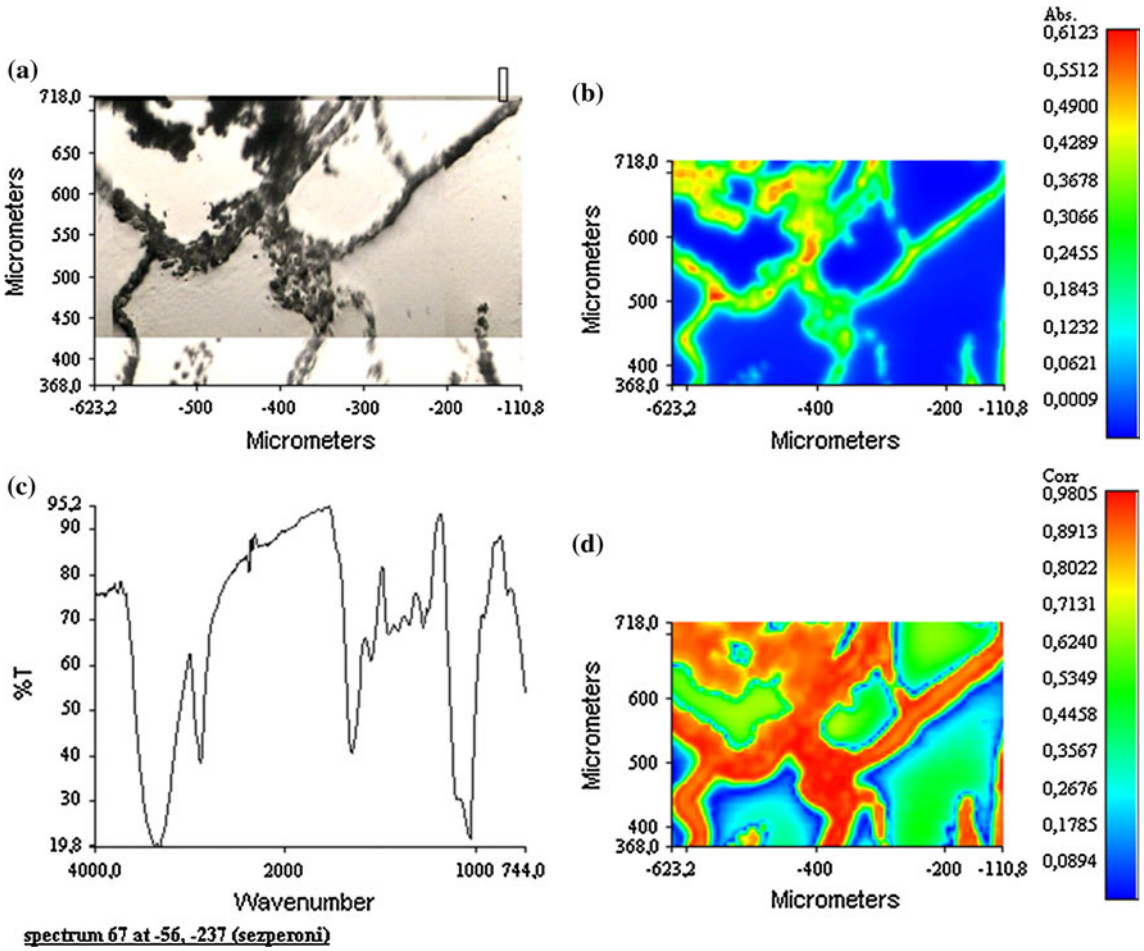

Fig. 8 Chemical imaging investigation on the F3 sponge, cross-linked with TGase: optical image (**a**), chemical map (**b**), medium spectrum (**c**) and correlation map (**d**)

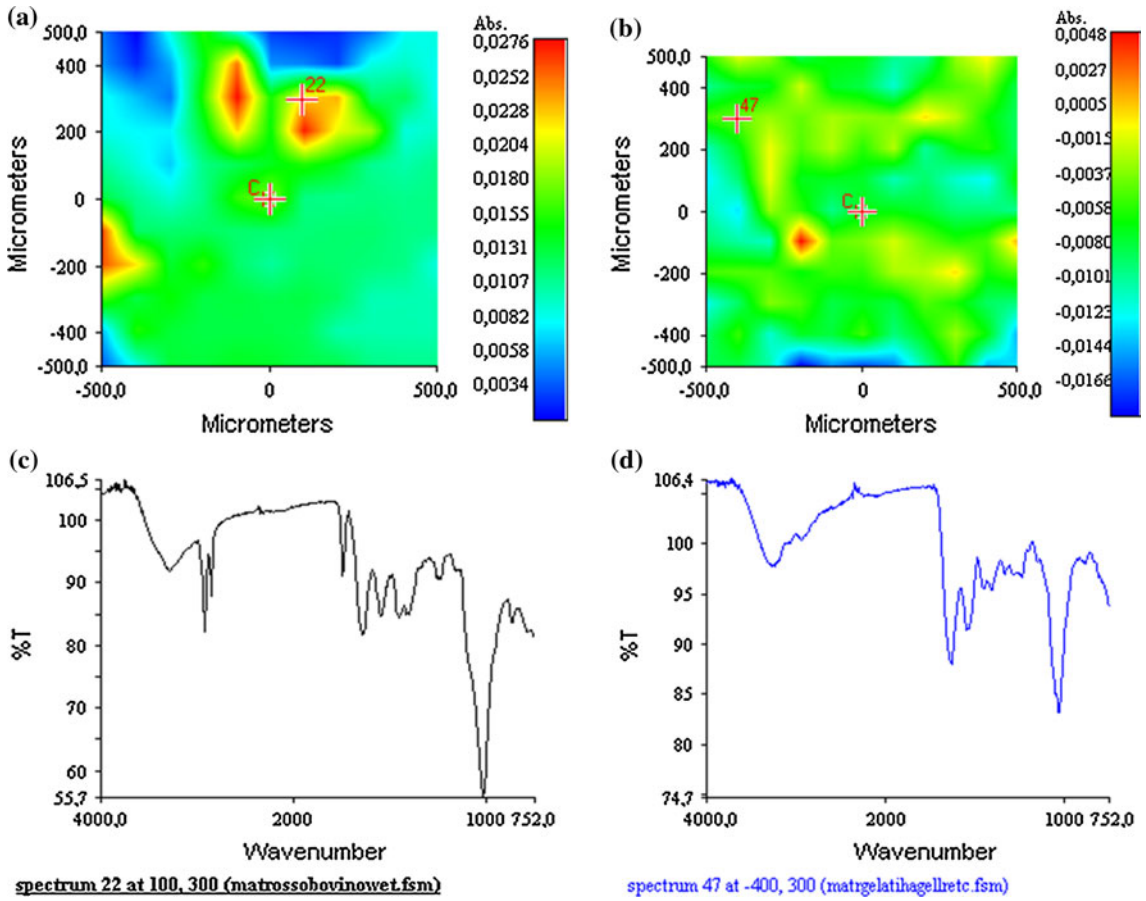

Fig. 9 Chemical map (**a**, **b**) and medium spectrum (**c**, **d**) of calf spongy bone (**a**, **c**) and composite scaffold (**b**, **d**)

interactions among the components of the blends, that made difficult the movements of the protein chains.

DSC thermograms of the sponge F3 after the cross-linking treatment and of natural spongy bone were also acquired. Before analysis, both samples were washed repeatedly with physiological solution and with bi-distilled water; then fractured in liquid nitrogen and finally dried at room temperature. The thermogram of natural bone (Fig. 6) showed an endothermic event between 120 and 160°C, assigned to the thermal denaturation of bone Col [20]. The thermogram of the cross-linked sponge (Fig. 6) showed an endothermic event, between 120 and 140°C, and a glass transition event, at 210°C (not shown): the first event, similar to that observed in the bone thermogram, could be attributed to the denaturation of the triple helix portions, produced during the reorganization induced by the enzymatic cross-linking treatment; the second event was related to the glass transition of the denatured protein chain. The event related to the thermal degradation of GE was not present, suggesting that the interactions between Gel and GE were not modified by the cross-linking treatment. A possible very strong interaction is the ionic bond between the carboxyl group of the GE repeating unit and the side amino group of a basic amino acid of the Gel peptide chain, like lysine, as shown in Fig. 2. Since the basic amino acids are not very abundant, but widely distributed in Col and Gel chains [17, 21], the ionic interactions with GE, which has a double-helix structure [22–24], might change the Gel conformation. In fact, at the low temperatures used for its gelling, Gel is quite disordered, although not really random coiled [17, 25]; the interactions established in the composites could produce a more structured conformation. Finally, a further ordering of Gel structure is caused by the cross-linking, as ascertained by other authors using various analytical techniques [17].

3.3 Mechanical characterization

The mechanical properties of the sponges were tested by means of the DMA measurements, from which the Young's modulus (E) was evaluated for all the sponges; its values are reported in Table 2. The values of E were not influenced by the frequency and increased with increasing the cooling rate for both the not cross-linked sponges and the cross-linked ones; the increase is greater for the latter. Indeed, for the sponge F1, the ratio between the modulus of

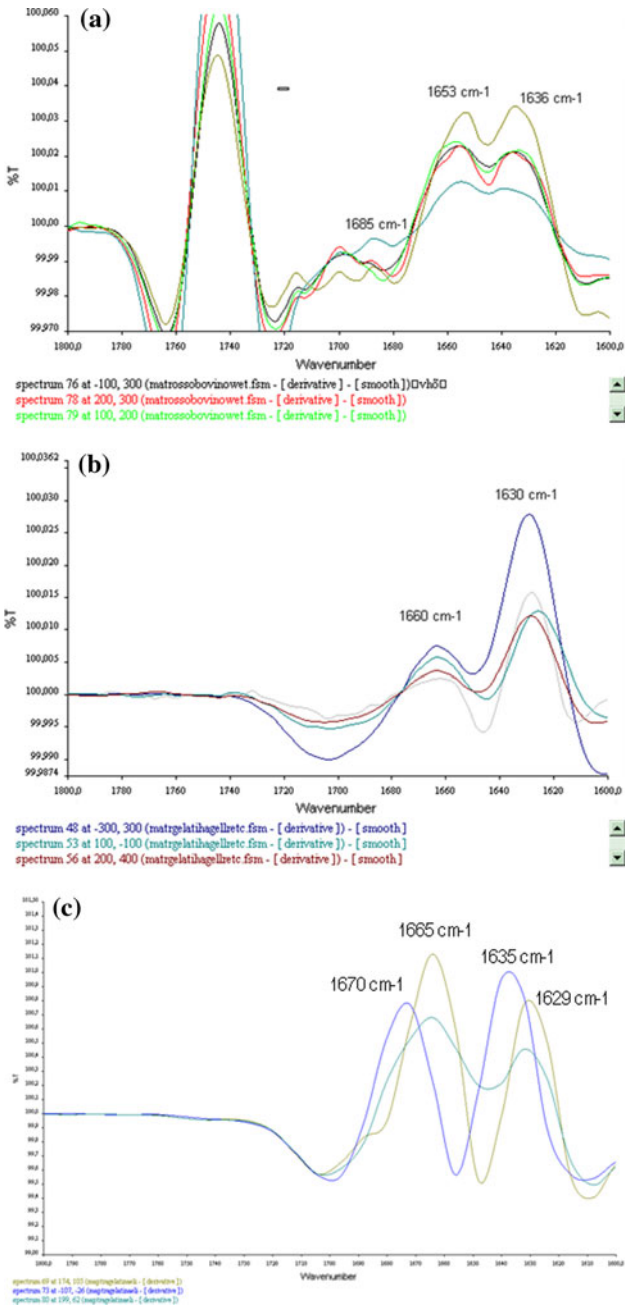

Fig. 10 Second derivative spectra of spongy bone (**a**), composite scaffold (**b**) and Gel (**c**)

the cross-linked sponge and that of the not cross-linked one was about 1.6, for F2 the ratio was about 2, and for F3 it was more than 3. Since the porosity of not cross-linked sponges became tighter with increasing the freezing rate (see Fig. 4a, c, e), the corresponding increase of the Young's modulus seems to be analogous to the inverse correlation between the longitudinal modulus and the porosity in human cortical bone [26]. Moreover, another cause can be invoked for the increasing of the elastic modulus: a more regular arrangement of the Gel and GE chains, induced by the lower gelling temperatures [17]. Finally, it can be observed that the value of the elastic modulus for the scaffold frozen in N_2 is comparable with the spongy bone (E = 20–500 MPa) [27].

On the basis of the results obtained in morphological, thermal and mechanical characterization, the sample F3 was chosen for further characterizations.

3.4 Infrared spectroscopy studies

The infrared spectrum obtained in ATR for non cross-linked F3 sponge is reported in Fig. 7 and it was compared with the infrared spectra recorded for Gel and GE samples, prepared in the same conditions, and for HA powder. Gel revealed absorption bands at: 3291.08 cm^{-1} (NH stretching), 1632.40 cm^{-1} (amide I, CO stretching), 1538.01 cm^{-1} (amide II, NH bending and CH stretching) and 1237.27 cm^{-1} (amide III, CN stretching and NH bending). GE showed absorption bands at: 1600.08 cm^{-1} (asymmetric COO^- stretching), 1407.29 cm^{-1} (symmetric COO^- stretching), and 1026.89 cm^{-1} (polysaccharide ring). In the HA spectrum, the phosphate band was evident between 900 and 1,200 cm^{-1} (PO_4^{3-} $\nu 1$ mode at 962.54 cm^{-1} and PO_4^{3-} $\nu 3$ mode at 1026.68 cm^{-1}). In the sponge, the addition of GE and HA to Gel caused a slight shift of the peak of amide I to lower wave number (1634.37 cm^{-1}); a more significant shift occurred for the band due to the symmetric stretching of GE COO^- (1,403 cm^{-1}), while the band due to PO_4^{3-} $\nu 1$ mode was no more detectable. These results demonstrated the presence of interactions among all the components of the blend. In particular, the shift of Am I confirmed the presence of interactions among the C=O of the protein chain and the calcium ions of HA; the shift of the band due to COO^- of GE demonstrated the presence of ionic interactions among Gel and the polysaccharide.

Chemical imaging investigation was performed in transmission mode on a thin section of the sponge cross-linked with TGase, cut through a microtome. The optical image (Fig. 8a) was characterized by the presence of empty spaces, delimited by branches of material that constitute the scaffold walls. The chemical map (Fig. 8b) faithfully reproduced the optical image, with very low levels of absorption in correspondence of the pores and higher absorption values on the scaffold walls. The FT-IR spectrum, acquired in a point of medium absorbance (Fig. 8c), showed the presence of the typical absorption bands of pure components. The correlation map (Fig. 8d) obtained by the correlation among the chemical map and the medium spectrum, showed a value close to 1, demonstrating the homogeneous distribution of the components in the scaffold and the absence of regions with a significant accumulation of one component or gradient of concentration.

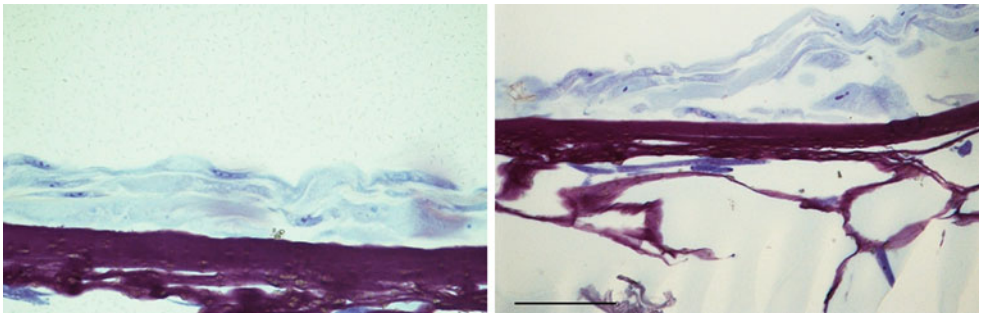

Fig. 11 Histological cross section of scaffold and hMSCs, after 21 days in culture

Finally, FT-IR chemical imaging investigation in μATR mode was performed on a section of calf spongy bone, dried by lyophilisation. The same analysis was performed on the scaffold and the results were compared. The medium spectrum of the two samples (Fig. 9) were very similar, even if in the bone map additional absorption peaks were present, due to the lipid component of the natural tissue analyzed.

The amide groups of proteins possess a number of characteristic vibration modes or group frequencies. Especially, the regions of the spectrum, in which the bands of amide I–III are present, are directly related to the polypeptide conformation. In particular, the amide I band in the bone spectrum is representative of the Col content and structure, and it is known that there are typical bands at 1,650–1,660, 1,630–1,640 and 1,680–1,700 cm^{-1}. To gain more detailed information regarding the secondary structural composition, we carried out the smoothing procedures and the second derivative of the maps was obtained, in order to resolve the overlapping components under the amide I contour bands at 1,685, 1,653 and 1,636 cm^{-1} (Fig. 10). The second derivative spectra obtained from the bone map (Fig. 10a) showed: the bands at 1,685 cm^{-1}, due to the degree of Col cross-linking in the natural bone; the band at 1,653 cm^{-1}, due to the organization as α helix of the protein molecule, and the displacement of this last band towards a lower frequency (1,636 cm^{-1}) [28].

Normally in the bone the absorption band for the C=O groups of Col fibrils (1,653 cm^{-1}) shifts at 1,645 cm^{-1}, as a consequence of bond formation among these groups and the calcium ions of HA. Similarly to natural bone, the derivative of the C=O band for the scaffold (Fig. 10b) showed the peak at 1,660 cm^{-1}, presumably related to α-helix conformation, and its shift towards lower frequencies (1,630 cm^{-1}). Differently, in the second derivative map of Gel (Fig. 10c), we observed a variability of the bands relative to the deconvolution of Am I. In particular, the peaks among 1,670–1,665 cm^{-1} and among 1,635–1,620 cm^{-1}, that can be attributed to β-turn conformation and to displacements of the unordered conformation, shifted towards lower frequencies, as a consequence of the high number of hydrogen bond interactions that the denatured protein can establish.

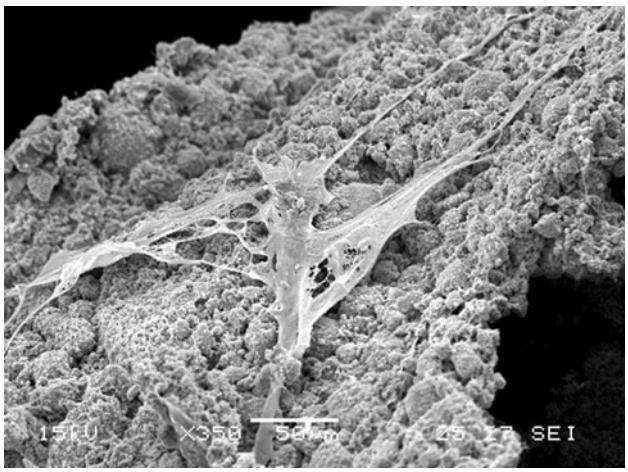

Fig. 12 SEM micrograph of hMSCs adhered on scaffold surface

These results demonstrated that the scaffold HA/Gel/GE, prepared according to method F3, had a chemical composition very close to that of the natural bone and, most importantly, the secondary structure of the scaffold protein component was similar to that of Col in the natural bone.

In conclusion, we can suggest that the stabilization of the protein produced by the polysaccharide component and the re-arrangement induced by the cross-linking with TGase, promoted the formation of interactions among protein C=O groups and HA, producing the formation of a bone-like matrix.

3.5 Cell proliferation

Cells plated became confluent in an adherent layer, contained a homogeneous population showing a fibroblastoid morphology. The immunophenotype, studied by cytometry, was positive for CD13, CD29, CD90 and did not express CD34, CD45 and CD14.

Figure 11 shows the histological cross section of scaffold and hMSCs after 21 days in culture. Cells fixed and stained by hematoxylin and eosin attached and proliferated with fibroblast like morphology. Cells were distributed on the surface and in the inner portion of scaffold.

The morphology of the cells grown on the F3 sponge was also investigated by SEM, after fixing cells with 2.5% glutaraldehyde solution, dehydrating the samples in a series of graded ethanol and finally drying them with a critical point apparatus. The cells grew favourably on the scaffold spreading out actively on the surface, as well as in the porosities (Fig. 12).

4 Conclusions

The results obtained in this work showed a high degree of interactions among the organic and inorganic components of the matrix, which produced bone-like scaffolds, in terms of chemical composition, as well as for the structural organization of the components. This positive result was confirmed by the good adhesion and proliferation on the scaffold of hMSCs.

In conclusion, the results of the morphological, physicochemical, mechanical and biological characterization of HA/Gel/GE sponges obtained by cooling in liquid nitrogen suggested their possible use as nanocomposite scaffolds for bone reconstruction.

References

1. Felsenberg D. Struktur und Funktion des Knochens. Pharm Unser Zeit. 2001;30:488–94.
2. Gagliardi M, Barbani N, Cristallini C, Guerra GD, Krajewski A, Mazzocchi M. Composites between collagen and hydroxyapatite. In: Ravaglioli A, Krajewski A, editors. Proceedings of the 11th Meeting and Seminar on: Ceramics, Cells and Tissues. Annual Conferences. Nanotechnology for functional repair and regenerative medicine. The role of ceramics as in bulk and as coating. Faenza (I) October 2007. Roma: CNR; 2008. pp. 182–91. ISBN 88-8080-085-X; 978-88-8080-085-9.
3. Barbani N, Rosellini E, Cristallini C, Guerra GD, Krajewski A, Mazzocchi M. Hydroxyapatite–collagen composites. Part I: can the decrease of the interactions between the two components be a physicochemical component of osteoporosis in aged bone? J Mater Sci Mater Med. 2011;22:637–46.
4. Rosellini E, Barbani N, Cristallini C, Guerra GD. Cross-linked hydroxyapatite–collagen composites as biomaterials for tissue engineering. In: Ravaglioli A, Krajewski A, editors. Proceedings of the 12th Meeting and Seminar on: Ceramics, Cells and Tissues. Periodical Conferences. Surface-reactive biomaterials as scaffolds and coatings: interactions with cells and tissues. Faenza (I) May 2009. Roma: CNR; 2009, pp.197–204. ISBN 978-88-8080-111-5.
5. Guerra GD. Composites of ceramics and glasses with synthetical and biological macromolecules. In: Ravaglioli A, Krajewski A, editors. Proceedings of the 12th Meeting and Seminar on: Ceramics, Cells and Tissues. Periodical Conferences. Surface-reactive biomaterials as scaffolds and coatings: interactions with cells and tissues. Faenza (I) May 2009. Roma: CNR; 2009, pp. 210–6. ISBN 978-88-8080-111-5.
6. Guerra GD, Cristallini C, Rosellini E, Barbani N. A hydroxyapatite–collagen composite useful to make bioresorbable scaffolds for bone reconstruction. Adv Sci Technol. 2010;76:133–8.
7. Neffe AT, Loebus A, Zaupa A, Stoetzel C, Müller FA, Lendlein A. Gelatin functionalization with tyrosine derived moieties to increase the interaction with hydroxyapatite fillers. Acta Biomater. 2011;7:1693–701.
8. Almora-Barrios N, de Leeuw NH. A density functional theory study of the interaction of collagen peptides with hydroxyapatite surfaces. Langmuir. 2010;26:14535–42.
9. Barbani N, Coluccio ML, Guerra GD, Krajewski A, Mazzocchi M, Ravaglioli A. Gellan gum–hydroxyapatite composites for the fabrication of scaffolds to be used in bone reconstruction. In: Ravaglioli A, Krajewski A, editors. Proceedings of the 9th Meeting and Seminar on: Ceramics, Cells and Tissues. Annual Conferences. Materials for Tissues Engineering, Chemistry and Microstructure: the Role for Ceramics. Faenza, (I) September–October 2004. Faenza: ISTEC-CNR; 2005, pp. 138–43. ISBN 88-8080-056-6.
10. Pranoto Y, Lee CM, Park HJ. Characterizations of fish gelatin films added with gellan and κ-carrageenan. LWT. 2007;40:766–74.
11. Folk JE, Finlayson JS. The ε-(γ-glutamyl)lysine crosslink and the catalytic role of transglutaminases. In: Anfisen CB, Edsall JT, Richards FM, editors. Advances in protein chemistry, vol. 31. New York: Academic Press; 1977. p. 1–133.
12. Chau DYS, Collighan RJ, Verderio EAM, Addy VL, Griffin M. The cellular response to transglutaminase-cross-linked collagen. Biomaterials. 2005;26:6518–29.
13. Barbetta A, Massimi M, Conti Devirgiliis L, Dentini M. Enzymatic cross-linking versus radical polymerization in the preparation of gelatin polyHIPEs and their performance as scaffolds in the culture of hepatocytes. Biomacromolecules. 2006;7:3059–68.
14. Barbetta A, Massimi M, Di Rosario B, Nardecchia S, De Colli M, Conti Devirgiliis L, Dentini M. Emulsion templated scaffolds that include gelatin and glycosaminoglycans. Biomacromolecules. 2008;9:2844–56.
15. Bertoni F, Barbani N, Giusti P, Ciardelli G. Transglutaminase reactivity with gelatine: perspective applications in tissue engineering. Biotechnol Lett. 2006;28:697–702.
16. Kim Y-J, Uyama H. Biocompatible hydrogel formation of gelatin from cold water fish via enzymatic networking. Polym J. 2007;39:1040–6.
17. Crescenzi V, Francescangeli A, Taglienti A. New gelatin-based hydrogels via enzymatic networking. Biomacromolecules. 2002; 3:1384–91.
18. Vogt S, Larcher Y, Beer B, Wilke I, Schnabelrauch M. Fabrication of highly porous scaffold materials based on functionalized oligolactides and preliminary results on their use in bone tissue engineering. Eur Cells Mater. 2002;4:30–8.
19. Mangano C, Scarano A, Iezzi G, Orsini G, Perrotti V, Mangano F, Montini S, Piccirilli M, Piattelli A. Maxillary sinus augmentation using an engineered porous hydroxyapatite: a clinical, histological, and transmission electron microscopy study in man. J Oral Implantol. 2006;32:122–31.
20. Kubisz L, Mielcarek S. Differential scanning calorimetry and temperature dependence of electric conductivity in studies on denaturation process of bone collagen. J Non Cryst Solids. 2005;351:2935–9.
21. Persikov AV, Ramshaw JAM, Kirkpatrick A, Brodsky B. Amino acid propensities for the collagen triple-helix. Biochemistry. 2000;39:14960–7.
22. Chandrasekaran R, Millane RP, Arnott S, Atkins EDT. The crystal structure of gellan. Carbohydr Res. 1988;175:1–15.
23. Chandrasekaran R, Puigjaner LC, Joyce KL, Arnott S. Cation interactions in gellan: an X-ray study of the potassium salt. Carbohydr Res. 1988;181:23–40.
24. Dentini M, Desideri P, Crescenzi V, Yuguchi Y, Urakawa H, Kajiwara K. Synthesis and physicochemical characterization of gellan gels. Macromolecules. 2001;34:1449–53.

25. Ross-Murphy SB. Structure and rheology of gelatin gels: recent progress. Polymer. 1992;33:2622–7.
26. Dong XN, Guo XE. The dependence of transversely isotropic elasticity of human femoral cortical bone on porosity. J Biomech. 2004;37:1281–7.
27. Azami M, Samadikuchaksaraei A, Poursamar SA. Synthesis and characterization of a laminated hydroxyapatite/gelatin nanocomposite scaffold with controlled pore structure for bone tissue engineering. Int J Artif Organs. 2010;33:86–95.
28. Chang MC, Tanaka J. FT-IR study for hydroxyapatite/collagen nanocomposite cross-linked by glutaraldehyde. Biomaterials. 2002;23:4811–8.